JOURNAL OF MATERIALS SCIENCE **35** (2000) 609 – 612

Self-monitoring of fracture and strain in titanium carbide reinforced silicon nitride ceramics

H. L. WANG, J. B. LI, J. F. LIU, Y. LI
State Key Lab of New Ceramics and Fine Processing, Tsinghua University, Beijing 100084, People's Republic of China
E-mail: ljb-dms@mail.cic.tsinghua.edu.cn

Si_3N_4 Ceramic Composites with TiC powder have been fabricated by gas-pressure sintering and their electrical conductivity has been investigated. The ceramic composites with different electrical resistivity consist of Si_3N_4 powder as an insulating matrix, and TiC as electrically conductive additive. Under tensile loading or compressive unloading, the $\Delta R/R$ of TiC/Si_3N_4 composites reversibly increased. Under compressive loading, the $\Delta R/R$ decreased gradually with the increasing of loading up to fracture. The results suggest the possibility of self-monitoring fractures and strains in the composites under tensile and compressive loading.

1. Introduction

The structural ceramics have been used in many important fields, but their application has been limited by the brittleness and fatal fracture. In order to make the structural ceramics more useful than before, some toughening methods have been adopted. Another method to increase the reliability of ceramics is to inspect the fractures and strains as it is at work so that the material may be repaired or replaced before it was destroyed. This kind of inspection needs sensors, especially strain sensors attached on critical places of the structure. However, common sensors have three deficiencies which are difficult to be overcome: too short the working-life, too limited the inspecting area and too costly. Now some structural ceramics have been endowed with self-monitoring ability. Such structural materials can detect its fractures and strains themselves instead of using additional sensors.

Atsumu Ishida *et al.* [1, 2] studied the change of electrical resistance in electrically conductive ceramic composites SiC/CaF_2 under tension and compression load and suggested the possibility of predicting fractures in ceramic composites. By applying mechanical load, electrical resistance of the composites increased up to fracture under tension while did not change or slightly decreased under compression. Shoukai Wang and D D L Chung [3] studied an SiCw/Si_3N_4 composite and found that the material was able to sense its own tensile strain, including reversible strain, but not compressive strain, so that this composite is a self-monitoring structural material.

N. Muto *et al.* [4] proposed a method to monitor the changes in electrical resistance in carbon–fiber–glass–fiber-reinforced plastics composites which was found to be a promising technique for foreseeing fractures and preventing fatal ones. Permanent, residual electrical resistance was found to be remain, and the changes in resistance depended on the maximum previous strain.

In the present work the granule TiC is taken as electrically conductive phase and added into Si_3N_4 to fabricate the electrically conductive ceramic composites with self-monitoring ability for the first time. In the case, the electrical resistivity of Si_3N_4 and TiC are 10^{11} Ω·m and 10^{-6} Ω·m, respectively. TiC has high hardness and high melting point, and can match Si_3N_4 in expansion coefficient and chemistry [5, 6].

2. Experiment

Si_3N_4 (Beijing Founder High-Tech Ceramics Company) and TiC (Zhuzhou Hard Alloy Factory) has an average size of 1.78 μm and 1.61 μm, respectively. The Si_3N_4 mainly consists of α-Si_3N_4 (95.5wt.%) and β-Si_3N_4 (3.5wt.%). The sintering additives, including Al_2O_3, Y_2O_3 and MgO are chemically pure. The ceramics is in a proportion of $Si_3N_4 : Al_2O_3 : Y_2O_3 : MgO = 100 : 8 : 2.5 : 1.5$ by weight. TiC is added to Si_3N_4 in 15, 20, 30, 35wt% based on the total weight of the above mixture. The powder according to the above proportions is ball-milled and mixed for 24 h in nylon jar. The resultant mixture is vacuum-filtrated, and dried at 60–80 °C, then sieved through 60 mesh. Green bodies are prepared by dry-pressing the above mixture at 10 MPa and then isostatic-pressing at 240 MPa. The samples have been sintered at 1825 °C for 1.5 h under nitrogen atmosphere with a pressure of 1MPa. The sintered samples have been machined into strength testing pieces of $3 \times 4 \times 36$ mm and toughness testing pieces of $6 \times 4 \times 36$ mm. The SEM testing pieces are polished, then etched in melted NaOH for 2 min.

Fracture strength is measured with a universal testing machine having a span of 30 mm at a cross head speed of 0.5 mm/min. K_{IC} is measured with the same machine by notch-girder method having a span of 24 mm at a cross head speed of 0.05 mm/min. The surfaces of the polished and the fractured samples are observed by scanning electron micrograph (SEM) to evaluate the microstructure of the composites.

Silver paint is sputtered on the both ends of the testing pieces, and calcined at 700 °C as electrodes. Then the electrodes are connected to the resistance meter (BY1941A) to measure the electrical resistance by the two-probe direct-current method during application of four-point bending and static compressing load at room temperature. The measurements of electrical resistance with applied load are made in two modes. First, the compressing load is applied in a single mode until the testing piece fractures. Second, repeated bending loads below the fracture strength are applied.

For compressive testing, specimens are $5.5 \times 4 \times 10$ mm and the axis of compression is along the longest dimension. For tensile testing, specimens are $6 \times 5 \times 55$ mm and the axis of tension is along the longest dimension, the above span is 20 mm, and the below is 40 mm. The strain is measured by a strain gage in tensile testing, and the fractional change of electrical resistance of the composites along stress axis is measured at the same time. For tensile testing, an electronic universal testing machine (DSS-25T) is used and the displacement rate is 0.05 mm/min. For compressive testing, the same machine is used and the displacement rate is 0.50 mm/min.

3. Results and discussion

3.1. Mechanical properties

On the X-ray diffraction patterns, β-Si_3N_4 and TiC can be found, i.e., α-Si_3N_4 have transformed into β-Si_3N_4, as shown in Fig. 1. Fig. 2 shows the results of the SEM observations on the polished and the fractured surfaces of the composites. The composites consist of β-Si_3N_4, TiC and Si-N-O glass. The grain size of Si_3N_4 increases remarkably. β-Si_3N_4 have grown as crystals with long pillar which have the length of 2–7 μm and the diameter of 0.2–3 μm, some of which are perfect hexagonal pillars. β-Si_3N_4 cluttered randomly and formed a framework, in which are isometric TiC grains filled with the grain size of 0.1–0.7 μm. Some of TiC grains are dispersed, and the others are agglomerated. The fracture strength and the fracture toughness of composites reach about 780.5 ± 65 MPa and 8.14 ± 0.7 MPa·$m^{1/2}$, respectively. The relative density of the samples reaches 96.5–98%.

3.2. Electrical resistivity

Electrical resistivity plotted as a function of TiC content in the TiC/Si_3N_4 composites gas-pressure sintered at 1825 °C is shown in Fig. 3. The increase of TiC content

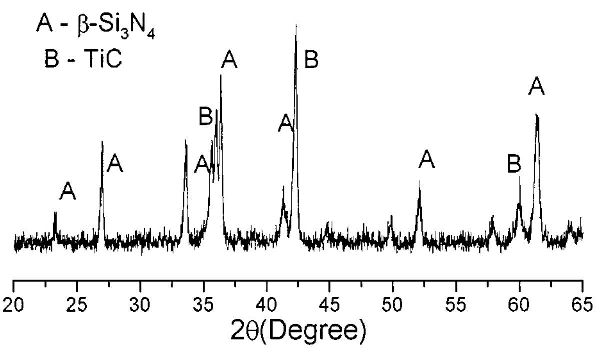

Figure 1 X-ray diffraction patterns of TiC/Si_3N_4 composites.

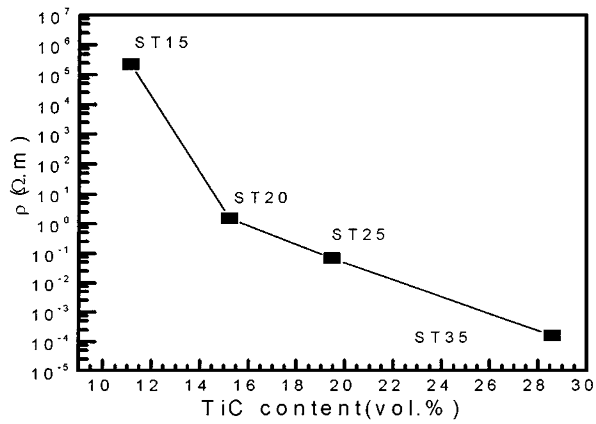

Figure 3 Electrical resistivity as a function of the TiC content in TiC/Si_3N_4 composites.

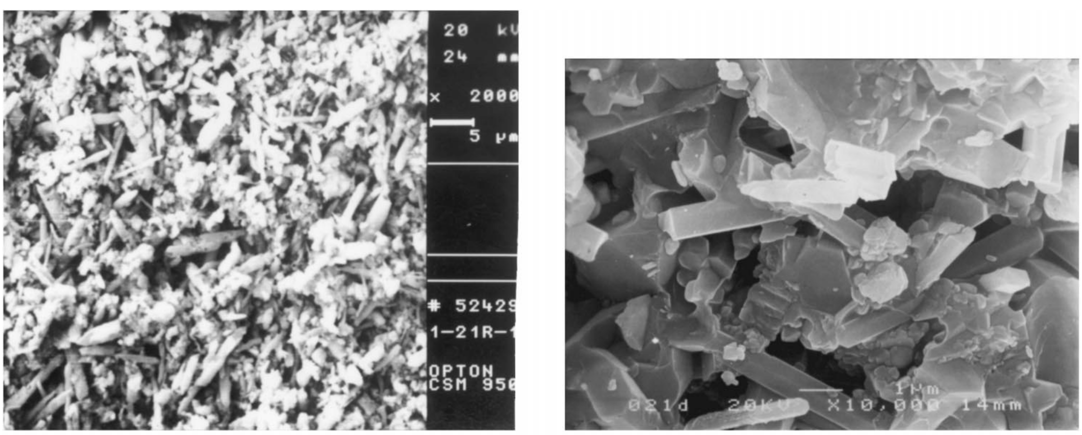

(a) (b)

Figure 2 SEM photographs of the microstructure of TiC/Si_3N_4 composites: (a) polished surface of the sample; (b) fractured surface of the sample.

from 15 to 35wt% results in a great decrease of electrical resistivity from 10^5 to 10^{-4} Ω·m. The electrical resistivity of ST20 is about 1–10 Ω·m.

According to the Percolation Theory of Scott Kirkpatrick [7], in a system consisting of insulating grains and electrically conductive grains only part of electrical conductive ones conduct electricity. The grains are assumed as points on the square lattice. As two electrically conductive grains take up two adjacent points, an electrically conductive path forms between them, then electricity could pass through. Unless the content of electrically conductive grains reach a critical value Vc—percolation threshold, the path will not come forth. The percolation threshold of the composites Vc equals to 16.45–18.50%.

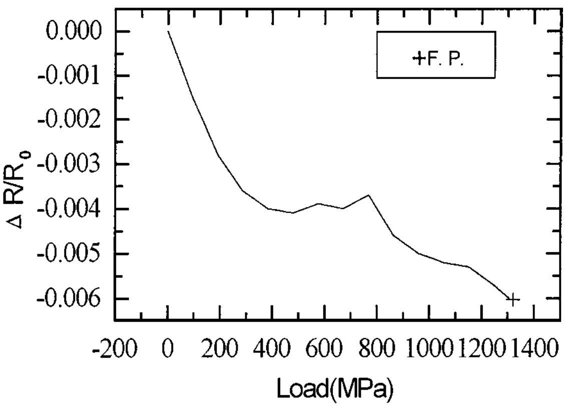

Figure 4 Ratio of decrease in electrical resistance to initial electrical resistance as a function of compressing load.

3.3. Change of R under load

Fig. 4 shows the relation between applied compressing load and ratio of change in electrical resistance to initial electrical resistance of Si_3N_4/20wt%TiC composite gas-pressure sintered at 1825 °C. After applying compressing load, the electrical resistance decreased by about 0.59–3.55% of the initial electrical resistance at fracture. The result indicates that the conduction paths have increased due to the closing up of electrically conductive grains when the compressing load is applied before fracture. The change of the the composites can also serve as a sensor similar to concrete containing short carbon fibers [8–10].

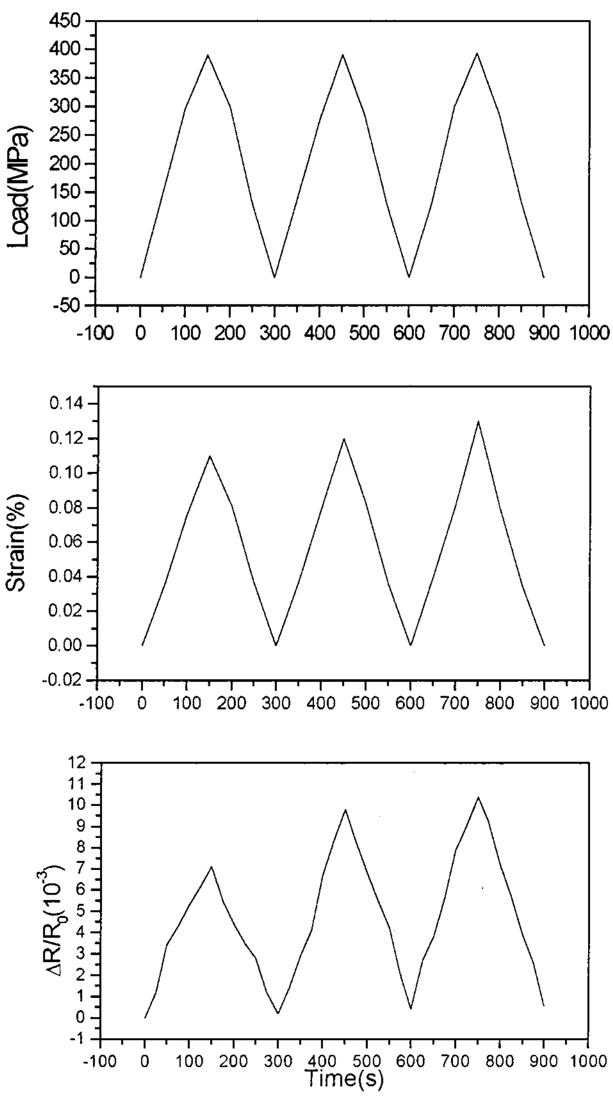

Figure 5 Variation of fractional electrical resistance increase ($\Delta R/R$), strain and stress during cyclic tensile loading at a stress amplitude equal to 50% of the fracture stress.

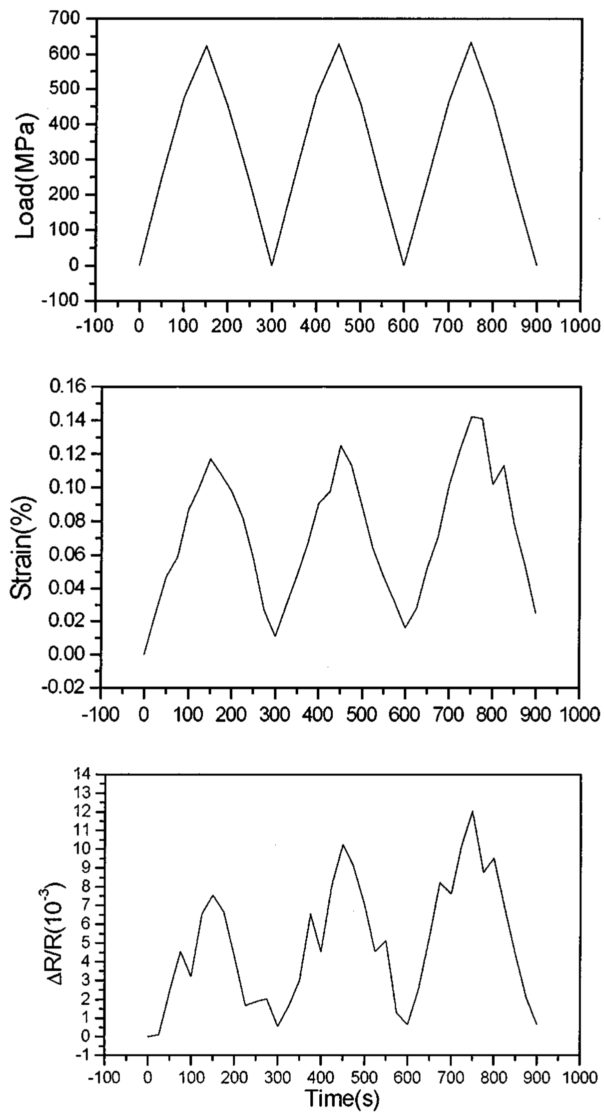

Figure 6 Variation of fractional electrical resistance increase ($\Delta R/R$), strain and stress during cyclic tensile loading at a stress amplitude equal to 80% of the fracture stress.

Fig. 5 gives the fractional resistance increase ($\Delta R/R$), strain and stress simultaneously obtained during cyclic tensile loading (displacement rate = 0.05 mm/min) at a stress amplitude equal to 50% of the fracture stress. The $\Delta R/R$ increases upon loading and decreases upon unloading in every cycle, which was within the stress regime in which the strain was reversible. Fig. 6 gives the similar results gained during cyclic tensile loading within the elastic regime at a stress amplitude equal to 80% of the fracture stress. The $\Delta R/R$ amplitude increases monotonically with increasing stress/strain amplitude so that $\Delta R/R$ amplitude. The change of the $\Delta R/R$ can be attributed to the rupture of electrically conductive paths due to the disconnecting of the electrically conductive grains and the $\Delta R/R$ provides an indication of the stress/strain

Under tension, the $\Delta R/R$ of TiC/Si_3N_4 composites reversibly increased during loading. The reversible effect is similar to that in concrete containing short carbon fibers [8–10]. The reversible strain and stress sensing ability of the ceramics comes from the reversible increase in the volume electrical resistivity. Such reversible increase is due to the disconnecting of electrically conductive paths during slight crack opening, which occurs upon tensile loading or compressive unloading.

4. Conclusions

TiC/Si_3N_4 composites with fracture strength of 780 MPa and fracture toughness of 8.14 MPa·$m^{1/2}$ have been fabricated by gas-pressure sintering process. In the composites TiC serves as electrical conductor and Si_3N_4 as insulating matrix. Under tensile loading or compressive unloading, the $\Delta R/R$ of TiC/Si_3N_4 composites reversibly increases due to the disconnecting of electrically conductive paths. Under compressive loading, the $\Delta R/R$ decreases gradually with the increasing of loading to fracture because of the increase of the conduction paths. The change of the electrical resistance can be used to predict the stress and fracture of the composites. The results suggest that the composites may be used as smart structural materials with self-monitoring ability for fractures and strains under tension and compression.

Acknowledgements

Financial support from the National Science Foundation of China (Grant No. 59432033) is acknowledged.

References

1. A. ISHIDA, M. MIYAYAMA and H. YANAGIDA, *J. Amer. Ceram. Soc.* **77** (1994) 1057–61.
2. A. ISHIDA, M. MIYAYAMA, A. KISHIMOTO and H. YANAGIDA, *J. Ceram. Soc. Jap.* **103** (1995) 576–581.
3. S. WANG and D D L CHUNG, *Smart Mater. Struct.* **6** (1997) 199–203.
4. N. MUTO, H. YANAGIDA, T. NAKATSUJI, M. SUGITA and Y. OHTSUKA, *J. Amer. Ceram. Soc.* **76** (1993) 875–879.
5. J. L. HUANG, M. T. LEE and H. HWALU, *J. Mater. Sci.* **31** (1996) 4899–4906.
6. CHIH-HUNG YEH and MIN-HSIUNG HON, *J. Amer. Ceram. Soc.* **78** (1995) 2395–2400.
7. SCOTT KIRKPATRICK, *Rev. of Modern Phys.* **45** (1973) 574–588.
8. CHEN PU-WOEI and CHUNG D D L, *J. Amer. Ceram. Soc.* **78** (1995) 816–818.
9. CHUNG D D L, *Smart Mater. Struct.* **4** (1995) 59–61.
10. CHEN PU-WOEI and CHUNG D D L, *ibid.* **2** (1996) 22–30.

Received 13 January
and accepted 22 July 1999